Contrib Mineral Petrol (1988) 100:35–46

Contributions to Mineralogy and Petrology

Constraints on the origin of Archean trondhjemites based on phase relationships of Nûk gneiss with H_2O at 15 kbar

A. Dana Johnston[1] **and Peter J. Wyllie**[2]

[1] Department of Geological Sciences, University of Oregon, Eugene OR 97403-1272, USA
[2] Division of Geological and Planetary Sciences, California Institute of Technology, Pasadena, CA 91125, USA

Abstract. We report the T-X(H_2O) phase relations for the trondhjemitic Nûk gneiss which comprises the principal component of the second phase of Archean (3.0–2.8 by) igneous activity in the Godthåb region of southwestern Greenland. A pressure of 15 kbar was chosen to place constraints on possible protoliths for trondhjemitic melts at lower crustal depths. Under H_2O-saturated conditions, a melting interval of ~135° C separates the solidus at ~610° C from the liquidus at 745° C. H_2O-saturation at 15 kbar occurs at approximately 15.5 wt % H_2O. The H_2O-undersaturated liquidus extends along a curved path from ~745° C at 15.5 wt % H_2O to ~1100° C at 2% H_2O. Lower H_2O contents were not investigated. At low H_2O contents (<6%) sodic plagioclase (Pl, An_{32}) is the liquidus phase followed at lower but still near-liquidus temperatures by quartz (Qz) and then garnet (Ga). At 6% H_2O, Ga replaces Pl on the liquidus and is joined at slightly lower temperatures by Pl and hornblende (Hb). The field for liquidus Ga extends to only ~7.5% H_2O where it is replaced by Hb which is the liquidus phase up to 13% H_2O. At all higher H_2O contents, epidote (Ep) is the first phase to crystallize, followed by biotite (Bi) at slightly lower temperatures. Following the standard inverse approach, the near-liquidus phase assemblages are interpreted as potential residues from which trondhjemitic melts could be extracted. At high melt H_2O contents (>7%), mafic residues consisting of some combination of Hb, Ga, Ep, and Bi are possible and could correspond to amphibolitic source rocks. At lower melt H_2O contents (<5%), possible residues consist of Na-Pl+Qz±Ga and could correspond to an earlier generation of tonalitic-trondhjemitic rocks. However, such residues would not impart the highly fractionated REE patterns characteristic of Archean trondhjemites. If a first generation of tonalitic-trondhjemitic melts was generated by higher pressure partial fusion of eclogite and emplaced at 55 km depth, it would crystallize to an assemblage consisting almost entirely of Na−Pl+Qz with highly fractionated REE patterns. These rocks in turn could be partially melted to yield a second generation of trondhjemites which would inherit the highly fractionated REE patterns because neigher Pl nor Qz is capable of significantly fractionating HREE from LREE.

Offprint requests to: A.D. Johnston

Introduction

In their 1976 paper, Barker and Arth stated: "The problem of the origin of trondhjemites and cogenetic tonalites and more mafic rocks has received little attention from petrologists and geochemists in recent years." There has been a resurgence of interest in these rocks because of their role as the principal components of the Archean terranes of all continents, along with associated but less abundant metabasalts. Barker and Arth (1976) noted that the Archean occurrences from part of a bimodal suite consisting of about 20% basalt and 80% tonalite/trondhjemite, with no rocks of intermediate composition. Barker, editor of a 1979 volume of *Trondhjemites, Dacites and Related Rocks,* reviewed the other occurrences of the tonalitic-trondhjemitic suite, and emphasized that trondhjemite is an abundant rock only in the Archean grey gneiss complexes. Kawakami and Mizutani (1984) estimated that trondhjemites and tonalites, typically metamorphosed to gneisses, constitute more than 80% of the high-grade gneiss terranes of the nine Archean cratons whose geology they reviewed, demonstrating their prominence in the development of the earliest continental crust. Many detailed field studies (e.g., McGregor 1979) and geochronometric studies (e.g., Jahn et al. 1984) demonstrate that the generation and emplacement of batholiths of trondhjemite and tonalite with associated eruptions of dacite and rhyolite is the second stage in the development of continental crust, following earlier voluminous outpourings of basalt and komatiite. Interpretation of the geology of greenstone belts and of the genetic relationships among mantle, komatiite, basalt, and tonalite-trondhjemite have been much debated, and it is essential that we understand the origin of tonalite-trondhjemite to gain insight into the origin and evolution of continental crust.

Origin of grey gneisses: approaches and hypotheses

One approach to the problem of early crustal genesis is to study the rocks in the field, to determine everything about the geochemistry of the rocks and minerals, to attempt to relate the rocks to each other, and to construct internally consistent petrogenetic schemes. This approach has been followed extensively. Another approach is to determine the phase relationships of the observed rocks and

the assumed magmatic sources under various conditions of pressure, temperature, and presence of various volatile components, and to apply the standard techniques of inverse and forward approaches to unravel the petrogenesis, or at least to apply constraints to petrogenetic schemes. This approach has been extensively pursued to elucidate the relationships between planetary mantles and basalts (Wyllie et al. 1981) and in attempts to constrain the origin of andesites and siliceous rocks associated with terrestrial subduction zones (e.g., Green 1980; Wyllie 1982; Johnston 1986). Less experimental attention has been directed towards the circumstances of the generation of the particular silicic rocks of the early continental crust.

Hypotheses for the origin of these silicic magmas fall into five categories: (1) Partial melting of eclogite or garnet granulite source materials with basaltic compositions (Arth and Hanson 1972; Condie and Hunter 1976; Compton 1978; Glikson 1979; Jahn et al. 1981), (2) partial melting of amphibolite with or without garnet (Barker and Arth 1976; Hunter et al. 1978), (3) fractional crystallization of basaltic magma (Arth et al. 1978), (4) direct partial melting of the mantle as has been implied on the basis of Sr isotopic arguments (Moorbath 1977), and (5) synmetamorphic Na-metasomatism of preexisting granites (Drummond et al. 1986). Jahn et al. (1984) have concluded that mechanism (4) is not plausible, because of this mechanism's inability to produce melts with either the major or trace element characteristics of Archean tonalite-trondhjemite series rocks (e.g., highly fractionated REE patterns, HREE depletion, $SiO_2 = 60$–75 wt %, $MgO = 0.5$–2.5%, $Na_2O/K_2O > 1.0$). Thus, apart from mechanism (5), the existence of a broadly basaltic protolith (including such diverse rock types as the sanukitoids reported from the Canadian Shield by Shirey and Hanson 1984) is apparently required for the generation of the silicic rocks that occupy the bulk of the shield areas on all of the continents. Moreover, the Sm-Nd data of Jahn et al. (1984) from the Baltic Shield of Finland convincingly demonstrate for the first time that, once formed, the first generation silicic rocks may themselves be remelted to produce additional generations of silicic rocks and that fresh pulses of basaltic material may be injected throughout the process. Thus, the generation of Archean continental crust was a complex process involving multiple melting episodes and a broad range of protolith compositions.

Previous experimental studies: constraints

Experimental studies have been published with direct relevance to hypotheses (1), (2), (3), and (4) listed above. Much effort has been expended on the forward and inverse approaches of experimental petrology for peridotite-basalt, and less for peridotite-komatiite. Incomplete data are available for combinations of the series gabbro-tonalite-trondhjemite-granite-H_2O. A few experiments apply to fractional crystallization of basaltic magmas. We are aware of no published experiments of the inverse type using natural trondhjemites.

Although anhydrous partial melting of peridotite (e.g., Jaques and Green 1979) is not capable of generating the silicic magmas of interest here, the much-debated hydrous peridotite melting experiments (e.g., Mysen and Boettcher 1975; Green 1976) demonstrate that the presence of water generates more siliceous liquids. In detail, however, the experimental melt compositions, coupled with the inability of peridotite (wet or dry) to generate melts with the appropriate trace element characteristics (Jahn et al. 1984), indicate that peridotite is not a suitable parent material for the generation of tonalite-trondhjemite series rocks under any set of physical conditions.

The conditions of partial melting of basaltic source material for the generation of tonalitic-trondhjemitic melts have been subjects of much debate (e.g., Barker and Arth 1976). Variables include the volatile content and depth of melting, and thus the mineralogical composition (e.g., basalt, amphibolite, garnet granulite, eclogite). Anhydrous basalt is not suitable, because neither plagioclase nor pyroxenes are capable of generating the highly fractionated, HREE-depleted REE patterns typical of Archean tonalite-trondhjemite series rocks; hornblende or garnet must be present in the residue after melting (Arth and Barker 1976). The low to moderate pressure (2–8 kbar) hydrous basalt melting experiments of Holloway and Burnham (1972) and Helz (1976) demonstrate the trondhjemitic-tonalitic melts are formed after 20–30% melting leaving hornblende in the residue. Similar siliceous melts with about 60 wt % SiO_2 have also been produced under anhydrous conditions from high-Al basalt (quartz eclogite) at high pressures (25–30 kbar) by Johnston (1986), and from basaltic andesite by Green and Ringwood (1968). About 30–35% melting leaves garnet, clinopyroxene and coesite in the residue. Melts approaching trondhjemite composition were calculated for about 10–15% melting of eclogite by Johnston (1986).

The formation of tonalite-trondhjemite melts by fractional crystallization of basaltic melts is more difficult to test. Nonetheless, an approximation of dry fractional crystallization of three lunar basalts at low pressures was achieved by Hess et al. (1975), who ran both cooling experiments and 'series-experiments'. At the low oxygen fugacities (Fe°-FeO) employed, all three compositions fractionated to ferrobasalt compositions after about 95% crystallization which, with further cooling, exsolved a second liquid similar in composition to granites. These liquids are more potassic than the tonalite-trondhjemite suite. Spulber and Rutherford (1983) found no liquid immiscibility in hydrothermal experiments on tholeiites, but the residual liquid after 90% crystallization is low K_2O-granitic, resembling plagiogranites and trondhjemites.

The H_2O-undersaturated liquidus surfaces for tonalite and granite presented by Stern et al. (1975) and Huang and Wyllie (1981) represent the inverse approach. The primary minerals on these surfaces are consistent with (1) the derivation of granites by partial fusion of crustal rocks, but not from peridotite (Wyllie 1984), and (2) the derivation of tonalite by partial fusion of crustal rocks but only at very high temperatures (or as crystal mushes), or of hydrous mantle peridotite but only at depths shallower than about 40 km (Nicholls and Ringwood 1973). Additional experimental data relevant to the possible sources of granitoid melts are available in isobaric H_2O-undersaturated liquidus boundaries for tonalite and granite at 15 kbar (Huang and Wyllie 1986), and for synthetic granite and granodiorite at 2 kbar and 8 kbar (Whitney 1975; Naney 1983). The effect on the near-liquidus mineralogy of varying water and oxygen fugacity in similar rock compositions has been investigated by Allen and Boettcher (1978, 1983) and Allen et al. (1975).

These experimental studies demonstrate that tonalitic-trondhjemitic melts may be generated by a variety of processes from a variety of source materials depending on such variables as the pressure, water content, and oxygen fugacity under which the process occurs. Although it is likely that all these processes have contributed to the generation of some trondhjemites, some may be ruled out for the generation of these rocks in Archean terranes. The absence of rocks with compositions between basalt and tonalite/trondhjemite needs explanation (Barker and Arth 1976). Liquid immiscibility would result in such a bimodality, but the relative volumes of the two compositions would be the reverse of that observed (Kawakami and Mizutani 1984). This bimodality also argues against an origin by differentiation of basalts, because the intermediate compositions that would surely have been produced are not found. Thus, it appears that the early crustal silicic compositions on Earth originated either by low to moderate pressure (<18 kbar) melting of hydrous basaltic (e.g., amphibolite) protoliths, or higher pressure, near-anhydrous melting of garnet-bearing basaltic materials (e.g., quartz eclogite).

As a step toward distinguishing between these various possibilities we have determined the phase relations of a natural trondhjemite from the Archean grey-gneiss terrane of southwestern Greenland at 15 kbar as a function of water content.

Starting material, the Nûk gneiss

A natural sample of the Nûk "granodioritic" gneiss, kindly provided by V.R. McGregor, was used in all experiments. This sample (#GGU 221121) is typical of the most voluminous phase of the type Nûk gneisses (McGregor, personal communication, 1985) which comprise the principal component of the second phase of Archean (3.0–2.8 bybp) igneous activity in the Godthåb region of southwestern Greenland. Ages, detailed field descriptions and inferences regarding the origin of the Nûk gneisses were reported by McGregor (1979), Bridgewater et al. (1976), and references therein. There is general agreement that the Nûk gneisses represent the metamorphosed equivalents of igneous precursors. Although these precursors have variously been described as tonalites, granodiorites and trondhjemites, sample 221121 is clearly a trondhjemite according to the criteria proposed by Barker (1979). An analysis of sample 221121 performed by the Geological Survey of Greenland together with an averaged microprobe analysis of a super-liquidus run product are given in Table 1.

Sample 221121 consists predominantly of sodic plagioclase and quartz with lesser amounts of biotite, epidote, and muscovite and trace quantities of anhedral opaque minerals and euhedral apatite. Foliation in the sample is defined by layers rich in phyllosilicates and composite quartz grains with undulose extinction. Biotite is pleochroic from straw-yellow to olive-green and often shares planar interfaces with discrete epidote grains which are pleochroic from tan to faintly yellow. Epidote also occurs along cracks within and grain boundaries between feldspars although it has a vermiform to granular texture in these settings.

The sample was crushed in a tungsten carbide shatter box and then ground by hand in an agate mortar and pestle under alcohol to an average grain size of 10 μm. Some grains as large as 40 μm persisted. The sample was dried at 110° C in a vacuum oven and stored in a desiccator between experiments.

Experimental methods

High pressure experiments were completed in a piston-cylinder apparatus with samples enclosed in gold capsules to minimize the effects of Fe-loss to the capsule. Phase assemblages exposed on polished surfaces of run products were determined and analyzed using standard methods with optical microscope, scanning electron microscope, and electron microprobe.

Table 1. Starting material: Nûk gneiss, trondhjemite #GGU 221121

Wt.%	A	B
SiO_2	71.09	72.21
TiO_2	0.20	0.23
Al_2O_3	16.45	16.15
Fe_2O_3	0.33	NA[a]
FeO	1.05	0.89[b]
MnO	0.03	0.04
MgO	0.60	0.58
CaO	2.76	2.90
Na_2O	4.93	4.73
K_2O	2.33	2.23
P_2O_5	0.05	NA
LOI[c]	0.46	NA
Total	100.28	100.00

A. Wet chemical analysis by the Geological Survey of Greenland (McGregor, pers. comm., 1985)
B. Average of four microprobe analyses of super-liquidus run product (Run #72), normalized to 100% to account for added H_2O.

[a] Not analyzed
[b] Total Fe as FeO
[c] Weight loss on ignition

Experimental procedures

Experiments were performed in a single-stage piston-cylinder apparatus (Boyd and England 1960), using a 0.5-inch-diameter piston. The apparatus was calibrated for pressure and temperature as described by Boettcher and Wyllie (1968). Temperatures, measured with W5Re/W26Re thermocouples, were controlled to within ±5° C of the set point by a digital, solid state controller manufactured by Eurotherm Corp., and were accurate to ±15° C. No correction for the effect of pressure on thermocouple emf was applied. Furnace assemblies consisted of an outer cylinder of NaCl containing the high purity graphite furnace tube which in turn contained an upper hollow NaCl cylinder, through which the thermocouple passed, and a lower solid NaCl pedestal containing the capsule (see below). All runs were brought to final pressure (15 kbar) with the hot piston-out procedure described by Boyd et al. (1967). Pressures listed in Table 2 are nominal, incorporate no corrections for friction, and are considered accurate to ±5%. Run durations varied from a minimum of 22 hours to a maximum of 90.5 hours. Oxygen fugacity was not buffered, but this should not significantly affect the liquid compositions because of the very low FeO content of the starting material (Table 1).

After loading of the dry rock powder and water, the gold capsule was sealed by arc-welding and then loaded into a die with powdered NaCl and pressed into a solid plug that fit in the bottom of the furnace tube. In this way, all empty space around the capsule was eliminated. The capsule was near the top of the pedestal, and care was taken that no more than 1 mm of NaCl was present between the capsule and the termocouple tip. After each run, the NaCl surrounding the capsule was dissolved in warm water and the capsule was dried and reweighed to check for leakage.

At the end of the majority of runs, the capsules were mounted in epoxy in small brass tubes which were then ground and polished to expose a surface for examination by SEM and electron microprobe. Near-solidus runs, particularly those in the water-saturated regions, plucked badly and good polished surfaces were not obtained. Some of these were crushed for examination by x-ray diffraction and by optical study of grains in immersion oils.

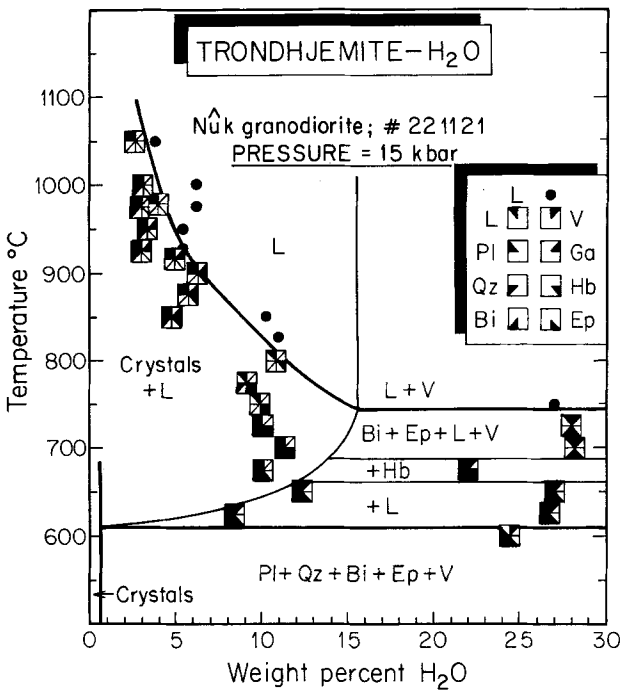

Fig. 1. Experimental results plotted from Table 2. The lines show bracketed phase boundaries for the solidus and liquidus, and for selected changes in the vapor-excess region. *Abbreviations: Pl* = plagioclase, *Qz* = quartz, *Bi* = biotite, *Ga* = garnet, *Hb* = hornblende, *Ep* = epidote, *L* = liquid, *V* = vapor

Analytical procedures

Phase identification was generally accomplished by back-scattered electron (BSE) imaging of the samples coupled with collection of EDS-spectra of individual grains using JEOL JSM-35A SEMs at Caltech and the University of Oregon. Additional BSE imaging as well as all quantitative analyses were performed on the JEOL 733 microprobes at Caltech and the University of Washington. All analyses were performed using a 5 nA beam current, and an accelerating potential of 15 kV. In an effort to minimize error due to element migration away from the electron beam, Na was always counted first. A defocussed beam was used for all glass analyses. Comparison of the microprobe analyses of a super-liquidus run product with the wet chemical analysis of the starting material (Table 1) suggests that this analytical procedure yielded satisfactory results. Standards consisted of a variety of natural minerals, synthetic oxides and pure metals. Data reduction was performed on-line using the procedure of Bence and Albee (1968).

Experimental results

The results of 32 runs at 15 kbar with the Nûk gneiss plus various H_2O contents are listed in Table 2 and plotted in Fig. 1. Figure 1 shows only the outline of the results for the T-X(H_2O) diagram, including the empirical boundaries with excess water. The runs are plotted for a total H_2O content equaling the amount added (Table 2) plus 0.5% corresponding to the amount already present in the rock (Table 1). The phases observed are listed around the key to the run points in Fig. 1; they were identified by a combination of optical methods and the analytical techniques described above. The presence of bubbles in the glass was taken as evidence for the presence of vapor under run conditions. Trace quantities of apatite and Al_2SiO_5-polymorph were also identified in near-solidus runs, but the data were inadequate for definition of their phase boundaries. Opaque minerals were not observed.

Table 2. Experimental results with trondhjemite-H_2O at 15 kbar

Run #	T (° C)	% H_2O[a]	Duration (hours)	Assemblage
71	1050	2.3	46.0	Pl,L
66	1000	2.7	70.5	Pl,Qz,L
73	980	3.6	43.0	Pl.L
69	975	2.6	47.0	Pl,Qz,L
68	950	2.9	46.0	Pl,Qz,Ga,L
70	925	2.7	49.0	Pl,Qz,Ga,L
62	920	4.8	68.0	Pl,Hb,Ga,L
63	900	5.8	44.0	Pl,Hb,Ga,L
64	875	5.2	90.5	Pl,Hb,Ga,L
65	850	4.3	72.0	Pl,Qz,Hb,Ga,L
45	800	10.4	24.0	Hb,L
46	775	8.9	48.5	Qz,Ep,Hb,L
48	750	9.6	49.0	Ep,Hb,L
50	725	9.7	46.0	Pl,Qz,Bi,Ep,Hb,L
51	700	10.8	45.5	Pl,Qz,Bi,Ep,Hb,L
52	675	9.6	50.0	Pl,Qz,Bi,Ep,L
55	650	11.8	46.5	Pl,Qz,Bi,Ep,L,V
54	625	7.9	46.5	Pl,Qz,Bi,Ep,L,V
38	725	27.5	24.0	Ep,Bi,L,V
39	700	27.7	24.0	Ep,Bi,L,V
42	675	21.5	46.0	Pl,Qz,Bi,Ep,Hb,L,V
43	650	26.6	46.0	Pl,Qz,Bi,Ep,L,V
44	625	26.1	70.5	Pl,Qz,Bi,Ep,L,V
47	600	24.1	68.5	Pl,Qz,Bi,Ep,V
72	1050	3.4	47.0	L
58	1000	5.7	24.0	L
59	975	5.8	46.5	L
60	950	4.9	67.5	L
61	925	4.9	72.0	L
56	850	9.7	23.0	L
49	825	10.5	24.0	L
37	750	26.8	22.0	L,V

[a] wt.% H_2O added to capsule; starting material contains additional 0.5% (LOI)

Abbreviations: Pl – plagioclase, *Hb* – hornblende, *Ep* – epidote, *Bi* – biotite, *Ga* – garnet, *Qz* – quartz, *L* – liquid, *V* – vapor

The solidus and the H_2O-saturated liquidus were bracketed as shown. These boundaries are assumed to be isothermal at this pressure. The H_2O-undersaturated liquidus was tightly bracketed, and extrapolated upward toward the high-temperature liquidus estimated for anhydrous granite (Stern and Wyllie 1973). The boundary of the subsolidus vapor-absent field was plotted on the basis of the 0.46% weight loss on ignition reported for the analyzed rock (Table 1). This positioning assumes that all H_2O is bound in the minerals biotite, muscovite, and epidote.

Vapor-present results

The runs in Fig. 1 show the sequence of mineral assemblage changes through the melting interval for experiments containing a vapor phase. The subsolidus assemblage matches the mineralogy of the original rock, apart from muscovite which is present in the rock but was not observed in the run products.

The subsolidus assemblage is joined by liquid in the temperature interval 600–625° C. Between 650° C and

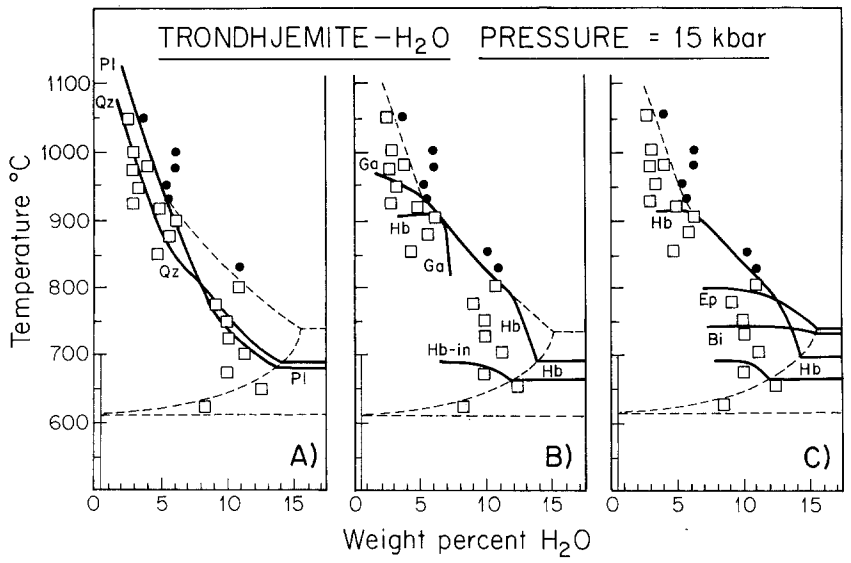

Fig. 2A–C. Phase boundaries based on runs plotted in Fig. 1. The mineral abbreviations identify the "mineral-out" curves, with the exception of hornblende which has both Hb-in and Hb-out phase boundaries

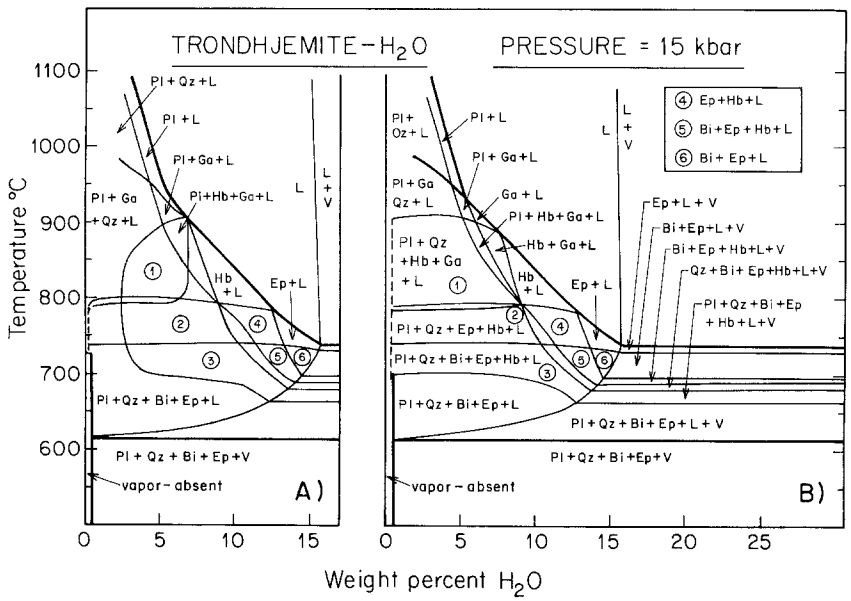

Fig. 3A, B. The effect of H_2O on the phase fields intersected by the Nûk Gneiss trondhjemite at 15 kbar, using the field boundaries determined in Fig. 2. **A** The interpretation in the low-H_2O region follows Naney's (1983) results for synthetic granodiorite at 8 kbar; **B** Our preferred interpretation, for reasons given in the text. For abbreviations see Fig. 1

675° C hornblende joins the assemblage, only to disappear in the temperature interval between 675° C and 700° C together with plagioclase and quartz. The assemblage Bi+Ep+L+V exists almost to the liquidus boundary, which is bracketed between 725° C and 750° C. The relative positions of isothermal phase boundaries for minerals that disappear within small temperature intervals in Fig. 1 have been interpreted on the basis of run data in the vapor-absent region and are shown in Figs. 2 and 3. Epidote rather than biotite is represented as the liquidus mineral.

The intersection of the isothermal liquidus line with the steeply dipping vapor-absent liquidus curve at 15.5% H_2O provides an estimate of the H_2O solubility in trondhjemite liquid at these conditions. The saturation boundary between this point and the solidus is loosely bracketed by the runs with and without vapor bubbles and is consistent with similar curves calculated at lower pressures by Robertson and Wyllie (1971).

Vapor-absent results

The near-liquidus phase relationships are well-constrained by closely spaced runs at temperatures extending to at least 100° C below the liquidus for three series of runs, with about 3% H_2O, 5% H_2O, and 10% H_2O. Phase boundaries for each mineral as defined by the observed phase assemblages are given in Fig. 2.

Boundaries for plagioclase-out and quartz-out are well defined in Fig. 2A, except that run #48 (750° C, 9.6 wt % H_2O) lacks quartz despite the other constraints that place it about 10° C within the quartz stability field. Fig. 2B shows the boundaries for hornblende-in and -out and their relationship to garnet-out. We have no runs in the low-H_2O region that define the low temperature stability limit of garnet (see the garnet-free subsolidus assemblage in Fig. 1). Finally, Fig. 2C examines the relative positions of the phase boundaries for the hydrous minerals, hornblende, epidote,

and biotite. The positions of these boundaries change relative to the vapor-present results. The upper boundary for hornblende-out rises to much higher temperatures than those for epidote and biotite, bringing hornblende to the liquidus for the temperature interval between about 775° C and 900° C. The results of vapor-present experiments do not discriminate between epidote and biotite as liquidus minerals, but the results with 10% H_2O suggest that epidote has a higher temperature stability than biotite in the vapor-present field. Note the way the Hb-out curve is constrained to cross over the Bi-out and Ep-out curves as it rises to the liquidus, creating a small interval with epidote on the H_2O-undersaturated liquidus as well as on the H_2O-saturated liquidus.

Our main experimental objective was to determine the primary minerals on the H_2O-undersaturated liquidus. Figure 2 shows a succession of primary minerals with increasing temperature: epidote, hornblende, garnet, and then plagioclase; there is a possibility that quartz might succeed plagioclase as the liquidus mineral before the anhydrous liquidus is reached and that biotite might precede epidote.

Interpreted phase diagram

The experimentally determined segments of the mineral phase boundaries from Fig. 2 are not very well constrained for extrapolation into the large vapor-absent region of crystals + liquid (Figs. 1 and 2). Examples of similar phase diagrams at 15 kbar are known for tonalite and muscovite-granite (Huang and Wyllie 1986), but these contain no epidote. The only relevant phase diagram containing epidote is Naney's (1983) 8 kbar T-X(H_2O) diagram for a synthetic hornblende-biotite granodiorite, which was based on many runs with H_2O contents down to 1 wt %. Using these studies as guides, we have constructed two interpretations, shown in Fig. 3, of how the phase boundaries might extrapolate into the vapor-absent region. The points of multiple intersection at ~800° C and 8 wt % H_2O are not constrained to meet in this special way by the runs but are drawn this way for simplicity (cf. Naney 1983, p. 1005); otherwise many additional small phase fields would be introduced in this region.

There are two important differences between the two interpretations shown in Fig. 3. The first concerns the stability of hornblende at low water contents. Figure 3A constructed using Naney's diagrams (1983, Figs. 3a, 4a) as a guide and shows the phase boundaries for hornblende-in and hornblende-out joining to form a continuous curve excluding hornblende from the low H_2O region. By contrast, Fig. 3B shows these curves extending separately all the way to the rock composition, similar to the biotite-out and epidote-out curves.

We prefer the interpretation shown in Fig. 3B for the following reasons: Consideration of Naney's (1983) 2 and 8 kbar data demonstrates that the hornblende stability field expands in temperature and migrates to lower H_2O contents as pressure is increased. The continued expansion of this field to 15 kbar would logically lead to the topology shown in Fig. 3B (Naney, pers. comm., 1988). Recent results by Rutter and Wyllie (1987), confirming that the phase boundaries for both hornblende and biotite in a tonalite have this configuration at 10 and 15 kbar, support this interpretation.

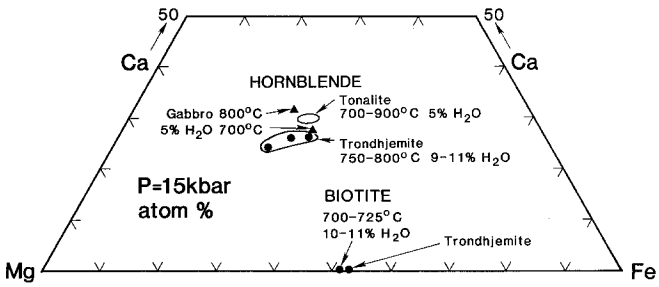

Fig. 4. Hornblende and biotite compositions compared to those crystallized from gabbro and tonalite at 15 kbar (Huang and Wyllie 1986)

The second important difference between the two interpretations shown in Fig. 3 concerns the points of multiple saturation along the H_2O-undersaturated liquidus. In Fig. 3B we show one point at ~900° C and 7 wt % H_2O where the melt is simultaneously saturated with respect to plagioclase, hornblende, and garnet. This point corresponds to run #63 which does contain these three phases. We consider it too much of a coincidence, however, for this point of multiple saturation to occur precisely at the pressure of 15 kbar selected for experimentation. Therefore we once again prefer the interpretation shown in Fig. 3B, with a short liquidus segment for primary garnet between plagioclase and hornblende. This is consistent with all other runs and implies that run #63 in fact plots just beneath the liquidus in the field for Pl + Hb + Ga + L.

According to Fig. 3B, on heating the vapor-free rock, which consists of the assemblage Pl + Qz + Bi + Ep, there is first a reaction generating hornblende (some melt would be produced if the formation of hornblende from biotite released H_2O), followed by the reaction of biotite to generate some H_2O-undersaturated liquid, and then the breakdown of biotite followed by epidote, with the formation of garnet associated with these reactions. At higher temperatures, near 900° C, the hornblende would also react, yielding additional H_2O for increased melting. Figure 2 shows that we have little information about the garnet phase boundary below the liquidus. This boundary is arbitrarily shown to pass through a point of multiple intersection in Fig. 3B, and the low temperature segment is drawn subhorizontally to indicate that its formation is coupled with the loss of biotite and epidote.

Consider the crystallization of a liquid with 5% H_2O with the aid of Fig. 3B. The phase boundaries suggest reaction relationships of the following types, in the sequence listed:

garnet + plagioclase + liquid = hornblende (1)
plagioclase + hornblende + liquid = epidote (2)
plagioclase + hornblende + liquid = epidote + biotite (3)
hornblende + liquid = biotite (4)

With excess H_2O, the hornblende-epidote reaction is reversed:

epidote + liquid + vapor = hornblende + plagioclase (5)

and then biotite is formed by reaction of the hornblende. Naney (1983) discussed similar reaction relationships in synthetic granodiorite-H_2O at 8 kbar.

Table 3. Microprobe analyses of glasses in experimental runs[a]

Run	65	70	68	69	66	71	72	51	50	48	46	45
T (° C)	850	925	950	975	1000	1050	1050	700	725	750	775	800
wt.% H_2O[b]	4.3	2.7	2.9	2.6	2.7	2.3	3.4	10.8	9.7	9.6	8.9	10.4
Assemblage	Gl,Ga, Pl,Qz	Gl,Ga, Pl,Qz	Gl,Ga, Pl,Qz	Gl,Pl, Qz	Gl,Pl, Qz	Gl,Pl,	Gl	Gl,Ep, Bi,Pl, Qz	Gl,Ep, Bi,Pl, Qz	Gl,Hb, Ep	Gl,Hb, Qz	Gl,Hb
# analyses	2	1	2	1	1	1	4	3	3	3	2	2
SiO_2	73.79	74.93	73.17	72.79	73.90	73.03	72.21	71.04	72.94	73.78	74.16	73.29
TiO_2	0.08	0.12	0.10	0.15	0.08	0.06	0.34	0.24	0.20	0.17	0.15	0.22
Al_2O_3	15.38	15.66	15.23	15.56	15.07	15.93	16.15	17.22	16.45	16.05	16.04	16.19
FeO[c]	1.14	1.17	1.00	1.21	0.80	0.58	0.89	1.24	1.09	1.13	1.01	1.17
MnO	0.02	0.10	0.05	0.00	0.04	0.00	0.04	0.10	0.05	0.07	0.02	0.09
MgO	0.43	0.56	0.61	0.72	0.63	0.60	0.58	0.40	0.32	0.34	0.25	0.31
CaO	2.49	2.15	2.67	2.39	2.70	2.66	2.90	2.95	2.49	2.56	2.55	2.81
Na_2O	4.03	2.39	4.49	4.49	4.44	4.89	4.73	4.33	4.09	3.56	3.46	3.64
K_2O	2.61	2.91	2.68	2.68	2.32	2.24	2.23	2.47	2.35	2.31	2.33	2.26
Total	100.00	100.00	100.00	100.00	100.00	100.00	100.00	100.00	100.00	100.00	100.00	100.00
Orig. total[d]	89.11	92.90	92.44	93.25	91.93	93.64	92.84	90.92	91.09	88.62	88.28	89.31

[a] Analyses are normalized to anhydrous totals of 100 wt. %. All analyses were obtained using a defocussed beam except run #70 for which a focussed beam was inadvertently used
[b] Wt.% H_2O added to capsule; glasses generally contain more H_2O due to crystallization of anhydrous phases
[c] Total Fe reported as FeO
[d] Original total of analysis before normalization

For abbreviations, see Table 2; Gl = glass

Table 4. Microprobe analyses of plagioclase in experimental runs

Run	65	70	68	69	66	71	51	50
T (° C)	850	925	950	975	1000	1050	700	725
Wt. % H_2O[a]	4.3	2.7	2.9	2.6	2.7	2.3	10.8	9.7
SiO_2	62.40	62.19	62.67	62.57	61.07	60.38	62.98	63.14
TiO_2	0.00	0.02	0.00	0.02	0.02	0.00	0.00	0.00
Al_2O_3	22.61	22.54	22.69	22.26	22.80	23.47	23.25	23.40
FeO[b]	0.09	0.09	0.05	0.26	0.09	0.08	0.14	0.02
MnO	0.04	0.08	0.00	0.00	0.00	0.00	0.00	0.00
MgO	0.00	0.00	0.00	0.11	0.03	0.03	0.00	0.05
CaO	4.98	5.27	5.23	5.99	5.99	6.84	4.62	4.88
Na_2O	8.79	8.76	8.81	6.35	7.80	7.28	8.95	8.74
K_2O	0.29	0.32	0.44	0.87	0.48	0.47	0.09	0.13
Total	99.20	99.28	99.88	98.43	98.27	98.54	100.16	100.43
Mol. % An	24	25	25	34	30	34	22	24

[a] Wt. % H_2O added to capsule
[b] Total Fe reported as FeO

Measured phase compositions

Selected electron microprobe analyses of phases in samples quenched from the vapor-absent region in Fig. 1 are listed in Tables 3–5, and illustrated in Figs. 4–6.

Glasses

Electron microprobe analyses of glasses are listed in Table 3 for 12 samples representing the range of temperatures investigated with approximately 3 and 10% H_2O. The analyses have been normalized to anhydrous totals of 100 wt % so they can be compared more easily with the bulk rock composition (Table 1) to assess the effects of crystallization on the melt compositions. We note, however, that despite using a low beam current (5 nA) and defocussed beam and always counting sodium first to minimize Na migration away from the electron beam, it is clear that some of the Na_2O analyses are still low. This problem is particularly apparent in the glass from run #70, which was inadvertently analyzed with a focussed beam, and the glasses containing the highest H_2O contents. The K_2O analyses may have been similarly affected but probably to a lesser degree.

Table 5. Microprobe analyses of mafic minerals in experimental runs

Phase	Hornblende			Epidote		Biotite		Garnet	
Run	48	46	45	51	50	51	50	70	68
T (° C)	750	775	800	700	725	700	725	925	950
Wt. % H_2O[a]	9.6	8.9	10.4	10.8	9.7	10.8	9.7	2.7	2.9
SiO_2	43.99	44.37	45.09	40.75	37.77	37.64	36.27	40.98	40.36
TiO_2	1.07	0.96	1.02	0.13	0.07	2.16	2.11	0.46	0.42
Al_2O_3	14.98	16.19	14.42	22.31	22.80	17.02	16.72	19.22	20.75
FeO[b]	13.34	14.15	12.55	11.27	12.42	18.92	18.35	21.33	18.76
MnO	0.15	0.20	0.17	0.21	0.32	0.15	0.18	0.63	0.71
MgO	10.82	9.54	12.25	0.04	0.00	10.08	9.81	10.33	9.95
CaO	8.71	8.57	8.57	21.88	22.79	0.10	0.14	5.98	7.71
Na_2O	2.86	2.85	2.71	0.07	0.00	0.21	0.41	0.14	0.09
K_2O	0.59	0.70	0.54	0.06	0.02	9.43	9.44	0.04	0.00
Total	96.51	97.58	97.32	96.72	96.22	95.72	93.43	99.11	98.75

[a] Wt. % H_2O added to capsule
[b] Total Fe reported as FeO

Despite the unfortunate problems with analyzing alkali-rich hydrous glasses noted above, some important conclusions may nevertheless be drawn from the data in Table 3. Perhaps the most striking feature of the glass analyses is the very limited range of compositional variability they display despite the broad range in percentage of crystals in the run products (up to ~40% in run #51) and the variety of coexisting crystalline phase assemblages. Moreover, the glass compositions do not differ greatly from the bulk trondhjemite. These observations stem from two basic causes. In the majority of the run products, the crystallized assemblages are dominated by sodic plagioclase and quartz and are thus very similar in composition to the bulk trondhjemite. In other runs that lack quartz and/or plagioclase but contain hornblende, epidote, or biotite (e.g., #45, #46, #48), the abundances of the mafic phases are very low (due to the low CaO, FeO*, and MgO abundances of the bulk rock), and thus their crystallization has only a limited influence on the compositions of the derivative melts.

Although the derivative melt compositions are clearly not identical to the bulk trondhjemite starting material, it is important to note that they are trondhjemitic nevertheless. This result suggests that melts with trondhjemitic major element compositions can be generated at 15 kbar by melting hydrous trondhjemite precursors. Trace element data pertaining to this possibility will be discussed in a later section.

Plagioclase

Plagioclase analyses (Table 4) were obtained for six samples with approximately 3% H_2O and two samples with about 10% H_2O. These analyses are of nearly pure albite-anorthite solutions ranging in composition from An_{30-34} near the liquidus at 3% H_2O to An_{22-25} at lower temperatures where it coexists with other Ca-bearing phases (hornblende and/or epidote).

Mafic minerals

Analyses of epidote, hornblende, and biotite were obtained from 2–3 samples each, all of which contained about 10% H_2O. These data together with garnet analyses from 2 samples containing about 3% H_2O appear in Table 5.

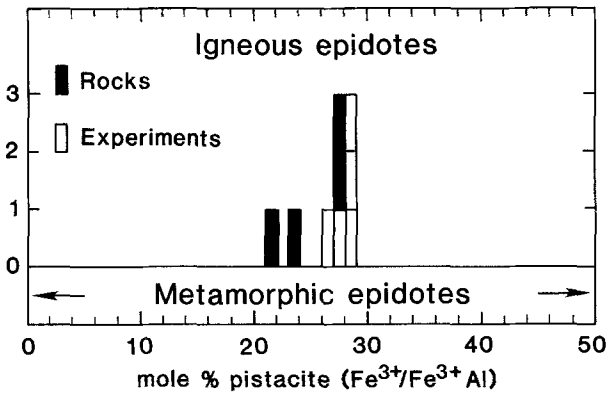

Fig. 5. Histogram showing magmatic epidote compositions from natural rocks (Zen and Hammarstrom 1984; Evans and Vance 1987) and experimental run products (this study and Naney 1983). Note the restricted range in compositions relative to that of metamorphic epidotes (Deer et al. 1962)

The hornblende and biotite analyses are from samples run at closely spaced temperatures and thus exhibit very limited compositional variability. The biotite has an atomic $Mg/(Mg+Fe^{2+})$ ratio of about 0.49 (Fig. 4) whereas a range of 0.54–0.63 is observed for hornblende. In Fig. 4, the hornblende analyses are compared with hornblendes crystallized from a gabbro and a tonalite at comparable pressures and temperatures but lower H_2O contents (Huang and Wyllie 1986). Despite the broad range in bulk compositions, the hornblende analyses are similar.

The observation of epidote in hypersolidus experiments in this study represents only the second report of epidote coexisting with melt in experimental run products (Naney 1983). In Fig. 5 our epidote analyses are compared to epidote in Naney's (1983) experiments and to examples of natural magmatic epidote from tonalitic plutons (Zen and Hammarstrom 1984) and dacitic dikes (Evans and Vance 1987). Despite the broad range of bulk composition (tonalite to trondhjemite), crystallization temperature (600–800° C), and H_2O contents (4 to 10 wt %) represented,

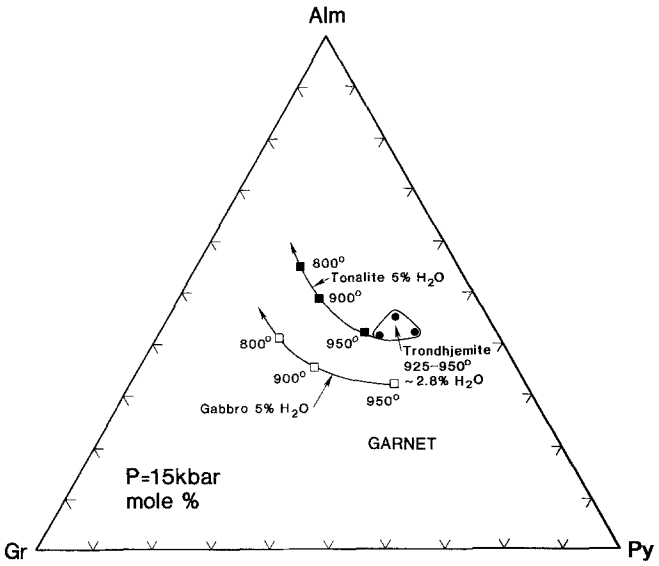

Fig. 6. Garnet compositions compared to those crystallized from gabbro and tonalite at 15 kbar (Huang and Wyllie 1986)

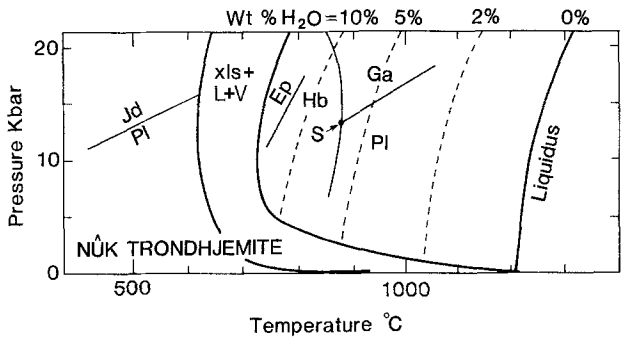

Fig. 7. Schematic results for the H_2O-undersaturated liquidus surface for the Nûk trondhjemite, based on the phase diagram in Fig. 3B and similar P-T projections for other rocks (Wyllie 1979, Figs. 19–21). The *heavy lines* represent the dry liquidus, the H_2O-saturated liquidus, and the solidus with H_2O. The liquidus surface is contoured by lines of constant H_2O content. Note point S which represents primary crystallization of hornblende, garnet and plagioclase

the analyses are remarkably similar, varying only from 21 to 29 mole % pistacite molecule; $Ps = Fe^{3+}/(Fe^{3+} + Al)$. Other examples of probable magmatic epidote, although not recognized as such at the time, support this observation (Hickling et al. 1970, Ps 31; Lee et al. 1971, Ps 27). The limited composition range of magmatic epidote was also recognized by Tulloch (1979, 1986) who noted that epidote in five compositionally diverse plutons he studied ranged only from Ps 25.2 to Ps 28.5. By contrast, epidote formed by subsolidus alteration of plagioclase (Ps 0–24) and biotite (Ps 36–48) is more variable in composition and overlaps only slightly with the compositions of magmatic epidote (Tulloch 1986). The data so far available suggest that epidote chemistry cannot serve as a sensitive indicator of crystallization conditions in magmas, but this may change as more natural examples of magmatic epidote are recognized and as more experiments are completed.

The garnet analyses are all simple three-component pyrope-grossular-almandine solutions (Table 5). In Fig. 6, these analyses are compared to the garnet crystallized from gabbro and tonalite bulk compositions at comparable pressures and temperatures but slightly higher H_2O contents (Huang and Wyllie 1986). The trondhjemite garnets at 925–950° C are similar to tonalite garnets at 950° C. Unfortunately, the temperature range represented by our garnet analyses is too limited to discern trends as a function of temperature.

Petrological applications

The results presented here represent the first of their kind for a trondhjemitic bulk composition and provide insight into processes that could generate trondhjemitic melts at depth in the crust. The experimental pressure of 15 kbar is attained at a depth of about 55 km in thickened crust of orogenic belts. The liquidus phase relations will first be examined to place constraints on permissible residues, and these will then be interpreted in light of the geochemical characteristics of Archean trondhjemites.

Inverse approach, possible mineral residues

Employing the standard inverse approach (Wyllie et al. 1981), the near-liquidus mineral assemblages are interpreted as potential residues from which a trondhjemite melt could be extracted. Implicit in this interpretation is the assumption that the composition of the melt just beneath the liquidus does not differ significantly from the bulk trondhjemite composition because so few crystals form. The glass analyses in Table 3 confirm this assumption and demonstrate, moreover, that the melt composition remains trondhjemitic as crystallization proceeds considerably further, at least to 100° C beneath the liquidus when the charge is about 40% crystallized (estimated mode of run #51). Mineral assemblages occurring well beneath the liquidus are therefore permissible residues from which trondhjemite melt could be extracted at 15 kbar. The data do not constrain the relative proportions of phases present in any real residue. It is only required that the mineral assemblage (and compositions) of a real residue correspond to one of those observed here.

Figures 1 and 3 show a variety of assemblages stable within 100° C of the H_2O-undersaturated liquidus of trondhjemite 221121. Although each of these represents a potential residue from which trondhjemite melt could be extracted, they only represent potential source rock assemblages if two conditions are met: (1) melting must not have been so extensive as to totally consume a mineral, and (2) the melt must not have been in a reaction relationship with any mineral. In either of these circumstances a mineral could be present in the source rock yet not appear near the liquidus of the derivative melt.

Figure 7 shows our estimate of the H_2O-undersaturated liquidus surface for the Nûk trondhjemite. This figure is based largely on the interpretation of our experimental results shown in Fig. 3B, and by analogy with similar diagrams constructed by Wyllie (1979, Figs. 19–21) using data from various sources. The liquidus surface is contoured by lines of constant H_2O content, and field boundaries separate the fields for crystallization of the primary minerals. Points on the contours and field boundaries at 15 kbar are defined in Fig. 3B. Lines drawn through these points by analogy with other rock systems provide the intersection point labeled 'S'. This represents the conditions of pressure,

temperature and H_2O content of liquid where trondhjemite melt is simultaneously saturated with garnet, hornblende, and plagioclase. The position of point 'S', although not well constrained, provides a minimum pressure for the occurrence of garnet on the liquidus. The small field for epidote at very high H_2O contents is consistent with our results at 15 kbar (Fig. 3B) and Naney's (1983) observation of subliquidus epidote in the synthetic granodiorite composition he studied at 8 kbar. The slope of the epidote-hornblende field boundary and the pressure of its intersection with the H_2O-saturated liquidus field boundary are not known and merit additional experimental study.

Figures 3B and 7 show that residues consisting of sodic-plagioclase with or without quartz and garnet are possibilities at 15 kbar and low H_2O contents (<5% in the liquid), although the temperatures required are high (>900° C). Such assemblages could correspond to the residues of melting earlier rocks with tonalitic to trondhjemitic compositions. At intermediate H_2O contents a variety of assemblages consisting of some or all of hornblende, garnet, Na-plagioclase, and quartz are possible residues. Such residues could result from a variety of processes. Assemblages containing sodic plagioclase could be produced by small to moderate degrees of partial melting of silicic precursors. Assemblages consisting of only hornblende + garnet could represent residues after large degrees of partial melting of silicic protoliths or more moderate degrees of melting of mafic precursors such as garnet-amphibolite. For liquids with very high H_2O contents (>9 wt %), residues consisting of hornblende and perhaps also epidote are possibilities.

Epidote crystallization in granitoid rocks

Naney (1983) confirmed experimentally the proposal advanced by a number of workers that epidote could occur in granitic magmas as a primary mineral. At 8 kbar, the solidus of the granodioritic composition studied by Naney was observed at 605° C. Epidote was observed to coexist with liquid to about 680° C in the H_2O-undersaturated region. For the trondhjemite at 15 kbar in Figs. 2C and 3B, epidote coexists with liquid to temperatures almost 200° C above the solidus temperature of 612° C. Furthermore, it has a small range (~750–775° C) as a primary liquidus mineral for bulk compositions with ≥13 wt % H_2O.

Zen and Hammarstrom (1984) noted that epidote in the natural samples they studied formed late, as a product of reaction between hornblende, plagioclase, and liquid producing epidote and biotite as products. This is the same reaction as (3) given earlier and is consistent with crystallization from a relatively H_2O-poor magma. By contrast, Hollister et al. (1987) noted that epidote in the Ecstall pluton is rimmed by biotite and suggested that it might not be a stable subsolidus mineral. No such reaction relationship is apparent in either our results at 15 kbar or Naney's (1983) results at 8 kbar; epidote persists as a stable subsolidus mineral in both studies.

At higher H_2O contents, epidote begins to crystallize closer to the liquidus (Fig. 3B). For bulk compositions containing 8–12 wt % H_2O, epidote crystallizes second after hornblende, whereas at higher H_2O contents it is the first mineral to crystallize. Thus, if abundant water were available, epidote phenocrysts might be expected in extrusive rocks such as were recently described in dacitic dikes by Evans and Vance (1987). On the basis of mineral equilibria calculations, Evans and Vance inferred high H_2O fugacities (about 6 kbar) during crystallization of their samples, although the total pressure they deduced (8–13 kbar) is somewhat less than that of the experiments reported here.

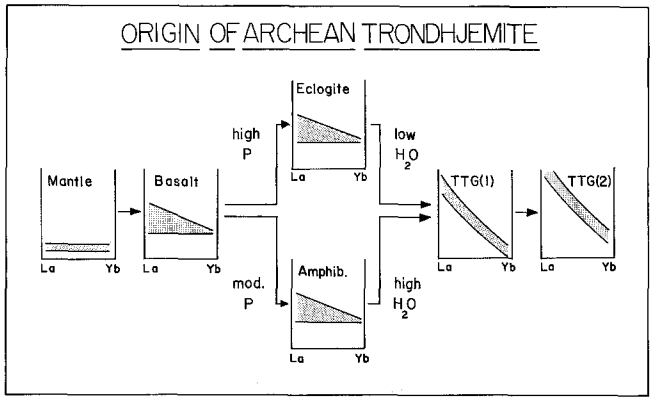

Fig. 8. Schematic multi-stage model for the origin of Archean trondhjemites that is consistent with available geochemical and phase equilibrium data. Partial melting of mantle peridotite generates a basaltic protocrust, which is soon transformed into either eclogite or amphibolite depending on pressure and the abundance of H_2O. These source materials are then partially melted to yield a first generation of tonalite-trondhjemite-granite (TTG) rocks with highly fractionated REE patterns. These TTG rocks can then be remelted to yield a second generation of TTG rocks that will inherit the fractionated REE patterns of their parent materials

Origin of Archean crust, other constraints

One of the intriguing characteristics of Archean tonalite-trondhjemite-granite (TTG) series rocks that distinguish them from TTG rocks of more recent time is their highly fractionated REE patterns ($(La/Yb)_n = 15$–50) which often also display HREE-depletion (O'Nions and Pankhurst 1974; Compton 1978; Jahn et al. 1984). These characteristics virtually require that garnet or hornblende made up a substantial percentage of the residue from which these melts were originally extracted.

From Figs. 3B and 7 it is clear that at 15 kbar, suitable residues are only in equilibrium with trondhjemitic melts containing abundant dissolved water (>5% in the melt fraction). However, this need not necessarily imply unusually abundant H_2O in the partially molten region as a whole if the melt accounts for only a small fraction of it. Lower crustal amphibolite or garnet granulite source rocks could generate melts with trondhjemitic major and trace element compositions. If sufficient water is not available, higher pressures are required to satisfy the REE constraint because of the positive slope of the plagioclase/garnet boundary on the H_2O-undersaturated liquidus of trondhjemite (Fig. 7) which requires increasing pressure with decreasing H_2O contents to remain in the garnet field. Under these circumstances nearly anhydrous eclogite in the form of tectonically overthickened crust or subducted oceanic crust would be a permissible source rock (cf. Johnston 1986).

The data presented here are also consistent with the multi-stage development model for the Archean crust in Finland developed by Jahn et al. (1984) on the basis of isotopic and trace element data. Their model, illustrated in Fig. 8, calls for at least three stages of crustal develop-

ment. First, basalts are formed by partial melting of peridotite and are soon transformed to garnet amphibolites or eclogites (depending on pressure and H_2O abundance) and remelted to yield a first generation of TTG composition rocks. After a considerable residence time, these TTG rocks are remelted to yield a second generation of TTG rocks with essentially identical major element compositions but highly evolved $^{143}Nd/^{144}Nd$ ratios.

Tonalitic/trondhjemitic melts generated by partial melting of amphibolite or eclogite would have highly fractionated REE patterns. If such melts were then emplaced at mid- to lower crustal levels, they would crystallize to assemblages consisting almost entirely of Na-plagioclase and quartz, the same phases that occur on or near the trondhjemite liquidus at low H_2O contents. Nevertheless, these plagioclase-quartz assemblages would contain the highly fractionated REE signature characteristic of their source. Subsequent melting of these rocks would generate melts with very similar major element compositions that would inherit the fractionated REE patterns of their source rocks because neither plagioclase nor quartz significantly fractionates heavy from light REE. Thus we would expect high negative slopes on chondrite-normalized REE plots for both first- and second-generation trondhjemites, although the REE abundances should be higher in second-generation products (Fig. 8).

Acknowledgements. This research was supported by the Earth Sciences Section of the National Science Foundation, Grant EAR83-41623, and the Early Crustal Genesis Project of NASA, NAG9-103. We thank V.R. McGregor, D. Bridgwater and the Geological Survey of Greenland for the rock samples and information, J.G. Arth and F. Barker for other trondhjemite samples and background information to guide our experiments, and A. Boudreau for help with the microprobe analyses. B.W. Evans, M.T. Naney, and an anonymous reviewer are thanked for their constructive reviews. Caltech Division of Geological and Planetary Sciences Contribution 4547.

References

Allen JC, Boettcher AL (1978) Amphiboles in andesite and basalt: II. Stability as a function of P-T-f_{H_2O}-f_{O_2}. Amer Miner 63:1074–1087

Allen JC, Boettcher AL (1983) The stability of amphibole in andesite and basalt at high pressures. Amer Miner 68:307–314

Allen JC, Boettcher AL, Marland G (1975) Amphiboles in andesite and basalt: I. Stability as a function of P-T-f_{O_2}. Amer Miner 60:1069–1085

Arth JG, Barker F (1976) Rare-earth partitioning between hornblende and dacitic liquid and implications for the genesis of trondhjemitic-tonalitic magmas. Geology 4:534–536

Arth JG, Hanson GN (1972) Quartz diorite derived by partial melting of eclogite or amphibolite at mantle depths. Contrib Mineral Petrol 37:161–174

Arth JG, Barker F, Peterman ZE, Friedman E (1978) Geochemistry of the gabbro-diorite-tonalite-trondhjemite suite of southwest Finland and its implications for the origin of tonalite and trondhjemite magmas. J Petrol 19:289–316

Barker F (1979) Trondhjemite: Definition, environment and hypotheses of origin. In: F Barker (ed) Trondhjemites, dacites and related rocks, Elsevier, Amsterdam Oxford New York, 659 p

Barker F, Arth JG (1976) Generation of trondhjemitic-tonalitic liquids and Archean bimodal trondhjemite-basalt series. Geology 4:596–600

Basaltic Volcanism Study Project (1981) Basaltic volcanism on the terrestrial planets. Pergamon, New York, 1286 p

Bence AE, Albee AL (1968) Correction factors for electron probe microanalysis of silicates and oxides. J Geol 76:382–403

Boettcher AL, Wyllie PJ (1968) The quartz-coesite transition measured in the presence of a silicate liquid and calibration of piston-cylinder apparatus. Contrib Mineral Petrol 17:224–232

Boyd FR, England JL (1960) Apparatus for phase-equilibrium measurements at pressures to 50 kilobars and temperatures up to 1750° C. J Geophys Res 65:741–748

Boyd FR, Bell PM, England JL, Gilbert MC (1967) Pressure measurement in single-stage apparatus. Carnegie Inst Wash Yrbk 65:410–414

Bridgewater D, Keto L, McGregor VR, Myers JS (1976) Archaean gneiss complex of Greenland. In: A Escher, WS Watt (eds) Geology of Greenland. Geol Survey of Greenland, 603 p

Compton P (1978) Rare earth evidence for the origin of the Nûk gneisses, Budsefjorden region, southern West Greenland. Contrib Mineral Petrol 66:283–294

Condie KC, Hunter DR (1976) Trace element geochemistry of Archean granitic rocks from the Barberton region, South Africa. Earth Planet Sci Lett 29:389–400

Deer WA, Howie RA, Zussman J (1962) Rock forming minerals, Vol 1, Ortho- and ring silicates. Longmans, London, 333 p

Drummond MS, Ragland PC, Wesolowski D (1986) An example of trondhjemite genesis by means of alkali metasomatism: Rockford granite, Alabama Appalachians. Contrib Mineral Petrol 93:98–113

Evans BW, Vance JA (1987) Epidote phenocrysts in dacitic dikes, Boulder County, Colorado. Contrib Mineral Petrol 96:178–185

Glickson AY (1979) Early Proterozoic tonalite-trondhjemite sialic nuclei. Earth Planet Sci Lett 15:1–73

Green DH (1976) Experimental testing of "equilibrium" partial melting of peridotite under water-saturated, high-pressure conditions. Can Mineral 14:255–268

Green TH (1980) Island-arc and continent-building magmatism – A review of petrogenetic models based on experimental petrology and geochemistry. Tectonophys 63:367–385

Green TH, Ringwood AE (1968) Genesis of the calc-alkaline igneous rock suite. Contrib Mineral Petrol 18:105–162

Helz RT (1976) Phase relations of basalts in their melting ranges at $P_{H_2O} = 5$ kbar. Part II. Melt compositions. J Petrol 17:139–193

Hess PC, Rutherford MJ, Guillemette RN, Ryerson FJ, Tuchfield TA (1975) Residual products of fractional crystallization of lunar magmas: An experimental study. Proc Lunar Sci Conf 6th, pp 895–909

Hickling HL, Phair G, Moore R, Rose HJ (1970) Boulder Crrek batholith, Colorado. Part I. Allanite and its bearing upon age patterns. Geol Soc Amer Bull 81:1973–1994

Hollister LS, Grissom GC, Peters EK, Stowell HH, Sisson VB (1987) Confirmation of the empirical correlation of Al in hornblende with pressure of solidification of calc-alkaline plutons. Amer Miner 72:231–239

Holloway JR, Burnham CW (1972) Melting relations of basalt with equilibrium water pressure less than total pressure. J Petrol 13:1–29

Huang W-L, Wyllie PJ (1981) Phase relationships of S-type granite with H_2O to 35 kbar: Muscovite granite from Harney Peak, South Dakota. J Geophys Res 86:1015–1029

Huang W-L, Wyllie PJ (1986) Phase relationships of gabbro-tonalite-granite-water at 15 kbar with applications to differentiation and anatexis. Amer Miner 71:301–316

Hunter DR, Barker F, Millard HT (1978) The geochemical nature of the Archean ancient gneiss complex and granodiorite suite, Swaziland: A preliminary study. Precambrian Res 7:105–127

Jacques AL, Green DH (1979) Determination of liquid compositions in high-pressure melting of peridotite. Amer Mineral 64:1312–1321

Jahn BM, Glikson AY, Pencat JJ, Hickman AH (1981) REE geochemistry and isotopic data of Archean silicic volcanics and granitoids from the Pilbara Block, Western Australia: Implica-

tions for the early crustal evolution. Geochim Cosmochim Acta 45:1633–1652
Jahn BM, Vidal P, Kroner A (1984) Multichronometric ages and origin of Archean tonalitic gneisses in Finnish Lapland: A case for long crustal residence time. Contrib Mineral Petrol 86:398–408
Johnston AD (1986) Anhydrous P-T phase relations of near-primary high-alumina basalt from the South Sandwich Islands: Implications for the origin of island arcs and tonalite-trondhjemite series rocks. Contrib Mineral Petrol 92:368–382
Kawakami SI, Mizutani H (1984) Geology and geochemistry of Archean crust and implications for the early history of the Earth. J Earth Sci Nagoya Univ 32:49–94
Lee DE, Mays RE, Van Loenen RE, Rose HJ (1971) Accessory epidote from hybrid granite rocks of the Mt. Wheeler Mine area, Nevada. US Geol Survey Prof Paper 750-C:112–116
McGregor VR (1979) Archean grey gneisses and the origin of the continental crust: Evidence from the Godthåb region, West Greenland, In: F Barker (ed) Trondhjemites, dacites and related rocks. Elsevier, Amsterdam Oxford New York, 659 p
Moorbath S (1977) Ages, isotopes and evolution of Precambrian continental crust. Chem Geol 20:151–187
Mysen BO, Boettcher AL (1975) Melting of a hydrous mantle II: Geochemistry of crystals and liquids formed by anatexis of mantle peridotite at high pressures and temperatures as a function of controlled activities of water, hydrogen, and carbon dioxide. J Petrol 16:549–593
Naney MT (1983) Phase equilibria of rock forming ferromagnesian silicates in granitic systems. Amer J Sci 283:993–1033
Nicholls IA, Ringwood AE (1973) Effect of water on olivine stability in tholeiites and the production of silica-saturated magmas in the island arc environment. J Geol 81:285–300
O'Nions RK, Pankhurst RJ (1974) Rare earth element distribution in Archean gneisses and anorthosites, Godthåb area, West Greenland. Earth Planet Sci Lett 22:328–338
Robertson JK, Wyllie PJ (1971) Rock-water systems, with special reference to the water-deficient region. Amer J Sci 271:252–277
Rutter MJ, Wyllie PJ (1987) Melting of tonalite and the origin of crustal granites. Trans Am Geophys Union 68:441
Shirey SB, Hanson GN (1984) Mantle-derived Archean monzodiorites and trachyandesites. Nature 310:222–224
Spulber SD, Rutherford MJ (1983) The origin of rhyolite and plagiogranite in oceanic crust: An experimental study. J Petrol 24:1–25
Stern CR, Huang WL, Wyllie PJ (1975) Basalt-andesite-rhyolite-H_2O: Crystallization intervals with excess H_2O and H_2O-undersaturated liquidus surfaces to 35 kilobars, with implications for magma genesis. Earth Planet Sci Lett 28:189–196
Tulloch AJ (1979) Secondary Ca-Al silicates as low-grade alteration products of granitoid biotite. Contrib Mineral Petrol 69:105–117
Tulloch AJ (1986) Comments on "Implications of magmatic epidote-bearing plutons on crustal evolution in the accreted terranes of northwestern North America" and "Magmatic epidote and its petrological significance". Geology 14:186–187
Whitney JA (1975) The effects of pressure, temperature, and $X(H_2O)$ on phase assemblages in four synthetic rock compositions. J Geol 83:1–31
Wyllie PJ (1979) Magmas and volatile components. Amer Miner 64:469–500
Wyllie PJ (1982) Subduction products according to experimental prediction. Geol Soc Amer Bull 93:468–476
Wyllie PJ (1984) Constraints imposed by experimental petrology on possible and impossible magma sources and products. Phil Trans R Soc London A-310:439–456
Wyllie PJ, Donaldson CH, Irving AJ, Kesson SE, Merrill RB, Presnall DC, Stolper EM, Usselman TM, Walker D (1981) Experimental petrology of basalts and their source rocks. Chapter 3 in Basaltic Volcanism on the Terrestrial Planets. Pergamon, New York
Zen E, Hammarstrom JM (1984) Magmatic epidote and its petrological significance. Geology 12:515–518

Received November 16, 1987 / Accepted May 16, 1988

Editorial responsibility: I. Carmichael